An antibiotic-sensing leader peptide regulates translation and premature Rho-dependent transcription termination of the *topAI* gene in *Escherichia coli*

Gabriele Baniulyte[1] and Joseph T. Wade[1,2]

[1]Department of Biomedical Sciences, School of Public Health University at Albany, Rensselaer, NY 12144, USA.

[2]Wadsworth Center New York State Department of Health, Albany, NY 12208, USA.

Abstract

Long 5′ UTRs in bacteria often contain regulatory elements that modulate expression of the downstream gene in response to environmental stimuli. In most examples of such regulation, the mechanism involves switching between alternative 5′ UTR RNA structures that impact transcription, stability, or translation of the mRNA. Here, we show that transcription of the *Escherichia coli topAI* gene is prematurely terminated by the termination factor Rho under standard laboratory growth conditions, and that this occurs as a result of translational repression. Regulation of *topAI* translation is controlled by a sensory ORF, *toiL*, located within the *topAI* 5′ UTR. We show that ribosomes translating *toiL* stall in a sequence-specific manner in the presence of specific ribosome-targeting antibiotics. Ribosome stalling at *toiL* induces conformational changes in the RNA structure of the *topAI* 5′ UTR, unmasking the *topAI* ribosome-binding site, thereby relieving translational repression and preventing premature transcription termination. Thus, *toiL* acts as a sensor of translation stress, leading to regulation of *topAI* at both the translational and transcriptional levels.

Introduction

There are two primary mechanisms of transcription termination in bacteria: intrinsic (also known as Rho-independent) and Rho-dependent. Intrinsic termination requires no protein factors other than the RNA polymerase (RNAP), and relies on a specific structure/sequence in the nascent RNA. By contrast, Rho-dependent termination requires a specific protein factor, Rho (Ray-Soni et al., 2016; Roberts, 2019). Rho is a hexameric, ATP-dependent helicase that binds nascent RNA and translocates along the RNA significantly faster than RNAP translocates along the DNA (Proshkin et al., 2010; Richardson, 2002); once Rho catches the RNAP it terminates transcription. Rho loading sites on nascent RNA are known as Rho utilization sites (Ruts). Although the RNA features that define Ruts are poorly characterized, Ruts are known to (i) be enriched for 'YC' dinucleotides, (ii) lack extensive secondary structure, and (iii) have a high C:G ratio (Alifano et al., 1991; Nadiras et al., 2018; Rivellini et al., 1991; Schneider et al., 1993). A Rho hexamer can stably bind a Rut containing a >58 nt stretch of RNA using the Rho primary RNA binding site (PBS), but requires ≥97 nts of transcribed RNA for successful termination (Hart and Roberts, 1991; Koslover et al., 2012; Zhu and von Hippel, 1998a, 1998b). Interaction of the Rho PBS with a Rut induces conformational changes in Rho, leading to closure of the hexameric ring (Lawson et al., 2016; Thomsen et al., 2016). PBS-bound RNA is then pulled through the central Rho pore, and interaction of this RNA with the secondary RNA binding site of Rho triggers ATPase and translocation activities (Skordalakes and Berger, 2006).

It has long been established that Rho does not terminate transcription in protein-coding regions (Adhya and Gottesman, 1978; Richardson, 2002). Several mechanisms have been proposed for why translating ribosomes prevent Rho termination, with all suggested mechanisms relying on the fact that transcription and translation are coupled processes in bacteria; indeed, recent studies have proposed that transcribing RNAP physically interacts with a ribosome (Fan et al., 2017; Kohler et al., 2017; McGary and Nudler, 2013; Saxena et al., 2018). One hypothesized mechanism by which translation inhibits Rho termination is simple occlusion of Ruts by elongating ribosomes (de Smit et al., 2009). An alternative hypothesis is that the RNAP-bound transcription elongation factor NusG binds ribosomal protein S10 (NusE), preventing interaction of NusG and Rho, a key step in transcription termination of some RNAs (Burmann et al., 2010; Chalissery et al., 2011; Saxena et al., 2018). While the NusG-S10 interaction may inhibit Rho at some loci, it is unlikely to prevent Rho termination of all translated RNAs, since only a subset of termination sites require NusG (Burns and Richardson, 1995; Peters et al., 2012; Shashni et al., 2014). Regardless of the mechanism, competition between ribosomes and Rho explains why Rho termination is often observed in the 3′ UTRs, but not in

actively translated regions (Burmann et al., 2010; Peters et al., 2012).

Recently, genome-wide studies of transcription termination identified large numbers of Rho termination sites in *Escherichia coli* (Cardinale et al., 2008; Dar and Sorek, 2018; Peters et al., 2009, 2012). These data indicate that the majority of Rho termination sites are in 3′ UTRs, or in non-coding RNAs that initiate antisense to protein-coding genes. Interestingly, ~3% of termination sites were proposed to occur in the 5′ UTR or coding region of protein-coding genes (Peters et al., 2012), suggesting that modulation of premature Rho termination is a widespread regulatory mechanism.

There are several characterized examples of genes that are regulated by premature Rho termination. These genes can be classified into two distinct groups based on the location of Rho termination: (i) termination in the 5′ UTR, and (ii) termination in the ORF. Rho termination in a 5′ UTR requires an accessible Rut, and termination is modulated via alternating terminator-antiterminator structures. Rho termination inside a coding region requires translation inhibition, typically through modulation of ribosome-binding site (RBS) accessibility. Rho termination inside a coding region also requires an accessible Rut; these Ruts are typically cryptic elements within the ORF that become exposed as a consequence of translational repression. Regulators of premature Rho termination events include small RNAs (sRNAs) (Bossi et al., 2012; Sedlyarova et al., 2016; Silva et al., 2019; Wang et al., 2015b), RNA-binding proteins (Baniulyte et al., 2017; Figueroa-Bossi et al., 2014), riboswitches (Bastet et al., 2017; Caron et al., 2012; Hollands et al., 2012), and small upstream ORFs (uORFs) (Ben-Zvi et al., 2019; Kriner and Groisman, 2015; Valle et al., 2019; Yanofsky, 2007).

In this work, we characterize the mechanism of premature Rho termination for the *topAI-yjhQ* operon transcript. The *topAI* and *yjhQ* genes encode a type II toxin-antitoxin system, where *topAI* encodes a topoisomerase A inhibitor, and *yjhQ* encodes the cognate antitoxin (Yamaguchi and Inouye, 2015). We establish that *topAI* gene is prematurely terminated by Rho, and show that this regulation requires translational repression. We further show that the long 5′ UTR of *topAI* encodes a regulatory uORF, *toiL*, that acts as a sensor for translation stress. We propose that stalling of the ribosome at *toiL* in response to translation stress induced by specific ribosome-targeting antibiotics causes structural rearrangements in the *topAI* 5′ UTR that unmask the *topAI* RBS for translation initiation, relieving both translational and transcriptional repression.

Results

Translational repression of *topAI* leads to intragenic Rho-dependent transcription termination

Genome-scale analysis of Rho termination identified a putative termination site in the coding region of *topAI* (Peters et al., 2012). The *topAI* gene has an unusually long 5′ UTR (171 nt) (Thomason et al., 2015). To independently assess whether Rho prematurely terminates *topAI* transcription, we constructed a truncated version of the *topAI* gene fused transcriptionally to the *lacZ* reporter gene, and measured expression in wild-type cells or cells expressing the R66S Rho mutant that is defective for RNA binding and termination (Baniulyte et al., 2017; Martinez et al., 1996). The reporter fusion included 42 nt of the *topAI* coding region followed by an in-frame stop codon and an independent RBS for the *lacZ* reporter gene. We observed ~7-fold higher expression in *rho* mutant cells than in wild-type cells (Fig. 1), consistent with a Rho termination site upstream of position 42 of the *topAI* gene.

The precise length and position of a *rut* is difficult to predict, since Rho binds RNA with relatively low specificity;

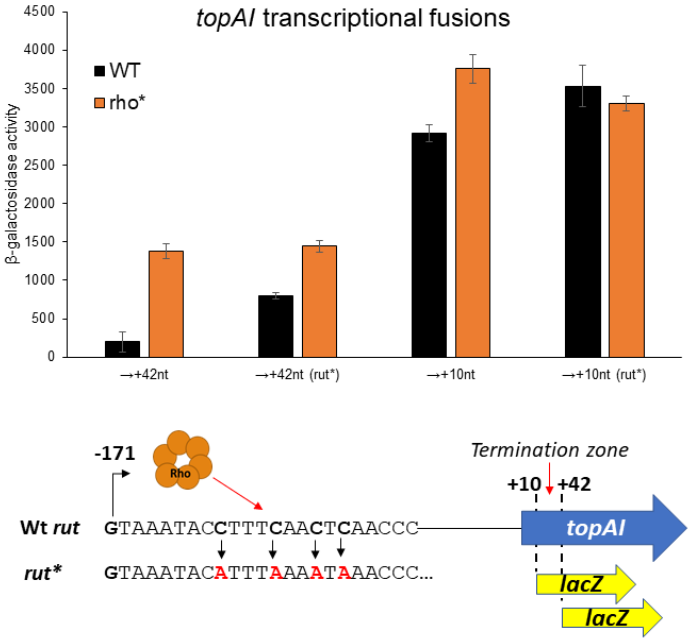

Figure 1. Translational repression of *topAI* leads to premature intragenic Rho-dependent transcription termination. β-galactosidase activity of truncated *topAI-lacZ* transcriptional fusions in wild-type (wt) MG1655 or *rho*(R66S) (*rho**) mutant cells. Constructs include 400 nt of the upstream sequence and up to 10-42 nt of *topAI* gene coding region, as indicated on the *x*-axis. The 4 nt mutation in the predicted *rut* site (*rut**) and other relevant features are indicated in the schematic diagram below corresponding graph. Error bars represent ±1 standard deviation from the mean (n = 3).

however, Rho is believed to favor pyrimidine-rich, unstructured RNA regions (Chhakchhuak et al., 2018; Nadiras et al., 2018). The most pyrimidine-rich region of the *topAI* is at the very 5' end. Mutating just four C residues in the Rho-terminated construct of *topAI* ('→+42', Fig. 1, left) caused a significant increase in expression in wild-type cells but no change in expression in *rho* mutant cells, consistent with increased transcriptional readthrough in wild-type cells. We conclude that the Rut includes the pyrimidine-rich sequence at the very 5' end of the *topAI* 5′ UTR.

To determine the location of the Rho termination zone, we measured transcriptional activity of a *topAI* fusion that included just 10 nt of the *topAI* ORF; there was no significant difference in expression between the wild-type and *rho* mutant strains with wild-type or *rut* mutant constructs of the short ('→+10', Fig. 1, right) *topAI* ORF fusions. This suggests that most of the transcription termination occurs between nucleotides 10 and 42 of the *topAI* coding region. We conclude that Rho is able to load onto the RNA early in the *topAI* 5′ UTR, but does not trigger termination for >180 nt.

Rho-dependent termination is tightly associated with translation; in protein-coding regions, translating ribosomes protect nascent mRNA and RNAP from Rho (de Smit et al., 2009). Given that Rho termination occurs within the *topAI* ORF (Fig. 1), we speculated that *topAI* is translationally repressed. To test whether *topAI* is actively translated, we constructed a *topAI-lux* translational reporter fusion and compared expression in wild-type and *rho* mutant cells. Although transcriptional repression of *topAI* is relieved in the *rho* mutant background (Fig. 1), *topAI* translation was strongly repressed in both wild-type and *rho* mutant cells (Fig. 2, left). These data suggest that Rho termination within the *topAI* coding region is a consequence of translational repression.

topAI translational repression is relieved by perturbation of global translation

Translation repression typically occurs by binding of a *trans*-acting factor (e.g. protein, sRNA, small molecule) overlapping the RBS (Breaker, 2018; Kriner et al., 2016). To identify *trans*-acting regulators of *topAI*, we used a genetic selection for spontaneous mutants with increased *topAI* expression. Briefly, the mutant selection used a *topAI-lacZ* construct in a Δ*lacZ* background; overnight cultures were plated on M9 + 0.2% lactose media that only allowed growth of spontaneous mutants with upregulated *topAI* expression (*cis*-acting mutants were discarded). We isolated 39 mutants with a mutant *rho* gene, suggesting that the screen was saturating. Additionally, we found 3 independent mutants that each carried single mutations in the 23S rRNA

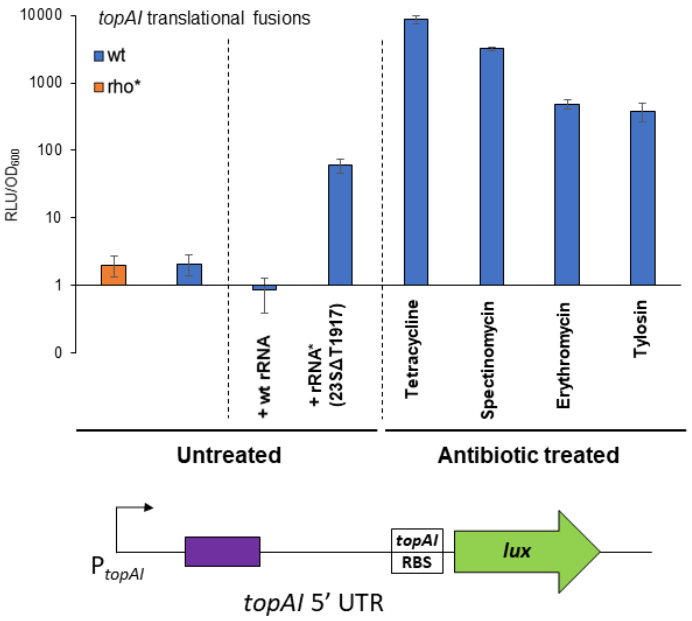

Figure 2. *topAI* translation is induced in response to ribosome defects. (*Left*) Luciferase activity of *topAI-lux* translational fusion construct in wild-type or *rho* mutant cells, as indicated in the legend. Cells were grown in LB medium until OD_{600}~1.0, a set of wt-background bacterial culture was treated with tetracycline (0.5 μg/ml), spectinomycin (90 μg/ml), erythromycin (100 μg/ml) or tylosin (400 μg/ml) (*right*). Activity was measure 90 min after antibiotic treatment. (*Middle*) Luciferase activity of *topAI-lux* translational fusion construct when either a wild-type rRNA or 23S rRNA mutant (ΔT1917) operons are overexpressed in *trans* from a pPro24 plasmid. rRNA operon was induced at OD_{600} ~0.1-0.2 by 12mM propionate; luciferase activity was measure after 4h. Reporter constructs include 400 nt of the upstream sequence up to the start codon of the *topAI* gene (see schematic diagram on the bottom). Error bars represent ±1 standard deviation from the mean (n = 3).

gene domains IV (*rrlA* ΔG1911, *rrlC* ΔT1917) or V (*rrlA* G2253T) (Table S1). Mutations in these regions are well characterized, and contribute to defective ribosome assembly and reduced binding of ribosome release and recycling factors (Agrawal et al., 2004; Barat et al., 2007). To test whether the rRNA mutations are sufficient to upregulate *topAI* translation, we expressed wild-type or mutant (23S rRNA ΔT1917) rRNA operons in *trans* and measured expression of the *topAI-lux* translational reporter fusion. Expressing the mutant 23S rRNA resulted in upregulation of *topAI*, whereas expression of wild-type 23S rRNA did not (Fig. 2, middle). Thus, the 7 nearly identical chromosomal rRNA operons cannot complement the dominant phenotype of the 23S rRNA mutant. We conclude that this effect on *topAI* expression is not simply due to a slight reduction in levels of active ribosomes.

Expression of toxin-antitoxin genes is often induced by environmental stresses (Page and Peti, 2016). We next aimed to identify an environmental condition(s) that *topAI*

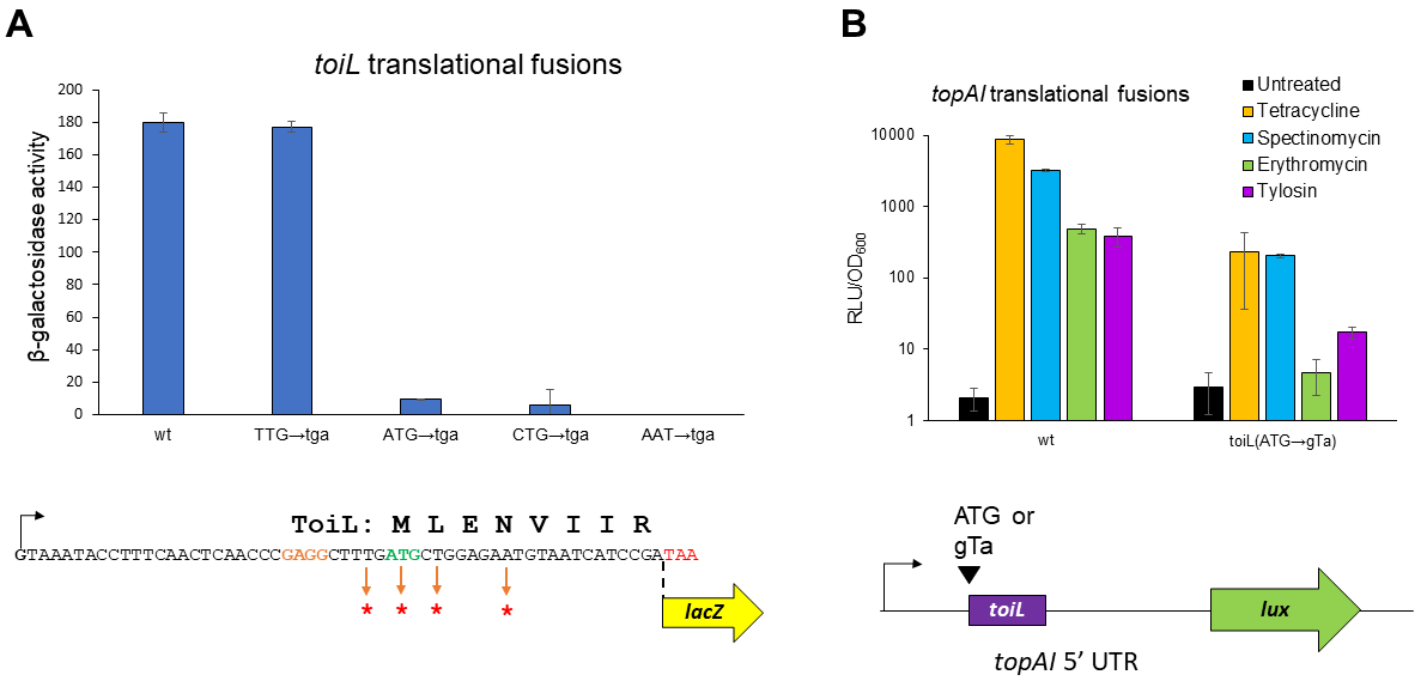

Figure 3. Expression of *toiL* is required for antibiotic mediated *topAI* regulation. β-galactosidase activity of *toiL-lacZ* (A) or luciferase activity of *topAI-lux* (B) translational fusion constructs. (A) Individual amino acid codons in *toiL* were replaced by stop codons ('tga'), as indicated in the schematic below the graph. (B) *toiL* start codon ('ATG') was mutated to 'gTa'. Cells were grown until OD600~1.0; tetracycline (0.5 μg/ml), spectinomycin (90 μg/ml), erythromycin (100 μg/ml) or tylosin (400 μg/ml) was added to one set of cultures. Activity was measure 90 min after antibiotic treatment Schematic representation of the reporter constructs used in (A) and (B) is depicted on the bottom. Error bars represent ±1 standard deviation from the mean (n = 3).

responds to. Given the effect of mutating 23S rRNA on *topAI* expression, we speculated that perturbing translation with ribosome-targeting drugs might have a similar effect. We tested a range of drugs (listed in Table. S2) at various sub-inhibitory concentrations. Tetracycline, spectinomycin, tylosin and erythromycin caused large increases in expression of the *topAI-lux* translational fusion (Fig. 2, right). Increased *topAI* mRNA levels upon short exposure to erythromycin, tylosin or clindamycin were also observed by Dzyubak and Yap (2016). It is possible that there are more antibiotics that could act in a similar way, or that the antibiotics we tested that had no effect (kasugamycin, gentamycin, amikacin, streptomycin, chloramphenicol, apramycin, hygromycin; Table S2) could work at different concentrations, as these drugs might also hinder expression of the reporter gene used in these experiments. Overall, *topAI* expression appears to be modulated by a subset of ribosome inhibitors, reinforcing the idea that expression of this toxin-antitoxin system responds to the translation status of the cell.

Expression of an uORF, *toiL*, is required for antibiotic-mediated *topAI* regulation

Long 5′ UTRs often contain regulatory elements such as uORFs that contribute to regulation of the downstream gene (Kriner et al., 2016). Given that *topAI* regulation responds to translation perturbation, we searched for a potential uORF that could act as a regulatory leader peptide for *topAI*. A uORF candidate, only 9 codons in length, 139 nt upstream of *topAI*, was identified by manually inspecting available genome-wide ribosome profiling data (Wang et al., 2015a; Weaver et al., 2019). A small peptide (*Mia*-127) with almost the same amino acid sequence (Fig. S1) and relative genome position was recently described in *Salmonella enterica* (Baek et al., 2017). To determine the frame and position of this uORF, which we renamed *toiL* (Topoisomerase Inhibitor Leader) in *E. coli* K-12, we used *toiL-lacZ* translational fusions to measure expression of this ORF. Replacing native codons with stop codons in the predicted CDS prevented expression of this fusion, unlike the equivalent substitution upstream of the ORF (Fig. 3A), supporting our ORF prediction. The first 7 amino acids of the *toiL* peptide are conserved across bacteria that encode the *topAI-yjhQ* operon (Fig. S1).

An ORF of such short length is most likely acting as a regulatory uORF. To test this, we asked whether *topAI* expression is induced by antibiotics if *toiL* is no longer translated. We mutated the start codon of *toiL* from 'ATG' to 'gTa' to preserve the predicted secondary structure of the 5′ UTR (Fig. S2A). The start codon mutation did not affect transcriptional readthrough before the predicted Rho

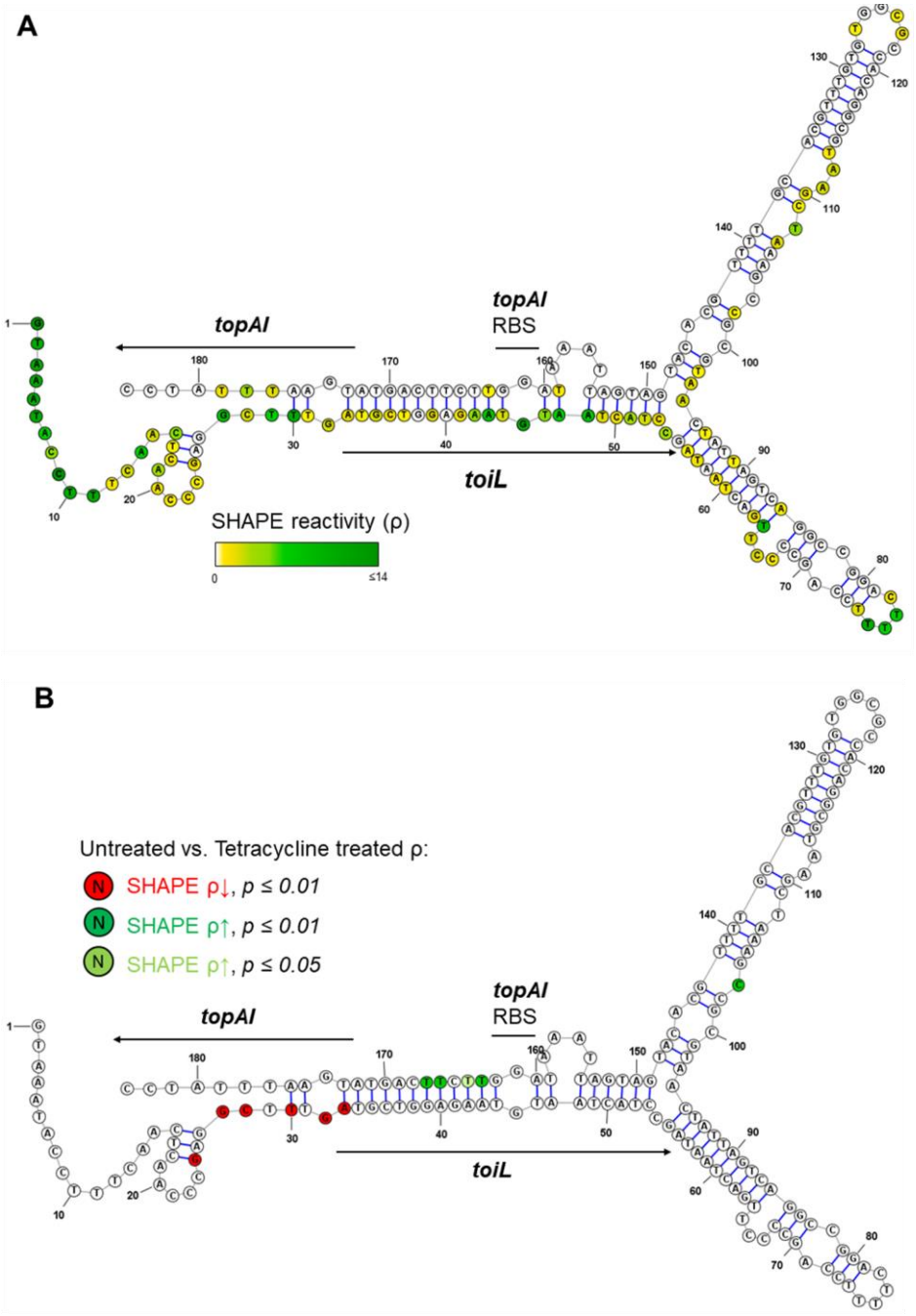

Figure 4. Structural changes in the 5′ UTR induced by antibiotic treatment. MFE structure of *topAI* 5′ UTR generated with mFOLD (Zuker, 2003). (A) In-cell SHAPE reactivities (ρ) of each base from an untreated sample are represented as a yellow-to-green gradient; white circles indicate no detected reactivity. (B) Bases with filled red or green circles indicate significant changes in SHAPE reactivity when cells were treated with 0.2 μg/ml of tetracycline for 90 min. Structures include *topAI* sequence from TSS; *toiL* (position 3-56) and *topAI* (from position 172) genes are indicated by arrows.

termination zone (Fig. S2B), indicating that it did not cause Rho termination at a more upstream site than in a wild-type construct. We measured expression of the *topAI-lux* translational fusion in the presence or absence of sub-inhibitory concentrations of ribosome-targeting drugs. When *toiL* translation was abolished, induction of *topAI* expression by the antibiotic treatments was greatly reduced (Fig. 3B), indicating that active translation of *toiL* is necessary for *topAI* regulation by ribosome-targeting antibiotics.

Drug-inhibited ribosome stalling within *toiL* leads to de-repression of *topAI* translation

Long 5′ UTRs that encode uORFs often utilize alternating RNA structures to modulate expression of the downstream gene (Kriner et al., 2016). For *topAI*, the regulatory element (i.e., a uORF) and the type of inducer (i.e. ribosome-targeting antibiotics) closely resembles the regulation of rRNA methyltransferase genes *ermB*/*ermC* (Subramanian et al., 2012), where stalling of the ribosome at the leader peptide in the presence of certain macrolides alters the downstream RNA structure, thereby facilitating *ermB*/*ermC* translation. Computational prediction of *topAI* 5′ UTR secondary structure suggests that the *toiL* ORF forms base-pairing interactions with the *topAI* RBS and start codon (Fig. 4A). We used in-cell SHAPE-seq (Watters et al., 2016a) to

complement the predicted structure and investigate any changes that occur upon exposure to tetracycline. The SHAPE reagent, 1M7, penetrates live cells and modifies the backbone of accessible RNA nucleotides. In the subsequent RNA library preparation steps, modified nucleotides block reverse transcription (RT), creating RT-stop points that are detected bioinformatically after the 1M7-treated and untreated libraries are sequenced. Lower SHAPE reactivity is an indication of increased base-pairing interactions or nucleotide occlusion by other cellular factors such as ribosome binding to the RBS.

Overall, the SHAPE-seq data and the computationally predicted structure are in good agreement (Fig. 4A). The beginning of the 5' UTR is highly reactive, as are predicted loops. Moderate reactivity in the *toiL* coding region is likely the result of translating ribosomes that temporarily disrupt the predicted long-range base-pairing interactions. Tetracycline treatment significantly changed reactivity in two distinct regions in the 5′ UTR in comparison to the untreated control: the *toiL* RBS became less reactive, whereas the *topAI* RBS became more reactive (Fig. 4B). We propose that, in the presence of tetracycline, ribosome occupancy at *toiL* increases due to stalling, which leads to a decrease in base-pairing between *toiL* and the *topAI* RBS. No significant changes in the *toiL* ORF region were observed, likely due to these nucleotides switching from being partly shielded by an actively translating ribosome and simultaneous base-pairing with *topAI* RBS (no treatment), to partial occlusion by a stalled ribosome (tetracycline treatment).

As a more direct test of ribosome stalling at *toiL*, we used a modified version of a previously described stalling reporter construct (Bailey et al., 2008). Macrolide-mediated induction of this reporter relies on ribosome stalling at the leader peptide *ermCL*. We designed a hybrid construct where the *topAI* 5′ UTR up to the 4th, 5th or 6th codon of *toiL* CDS is fused to the *ermCL* 10th codon and *ermCL* downstream sequence. These constructs include the downstream structural features from *ermCL* that are altered in response to ribosome stalling upstream. The 5 codon-long, wild-type version of the *toiL* fusion displayed greatly elevated expression in the presence of tetracycline, erythromycin or tylosin (Fig. 5), strongly suggesting ribosome stalling at *toiL*. These data are in good agreement with the observed decrease in SHAPE reactivity around the *toiL* RBS caused by tetracycline treatment (Fig. 4B) that suggests prolonged ribosome protection of RNA nucleotides at the RBS. The increases in stalling reporter expression upon drug treatment were largely abrogated in fusions up to the 4th or 6th codon of *toiL*, or when Val5 codon was mutated to Leu in the context of the 5-codon fusion (Fig. 5). This

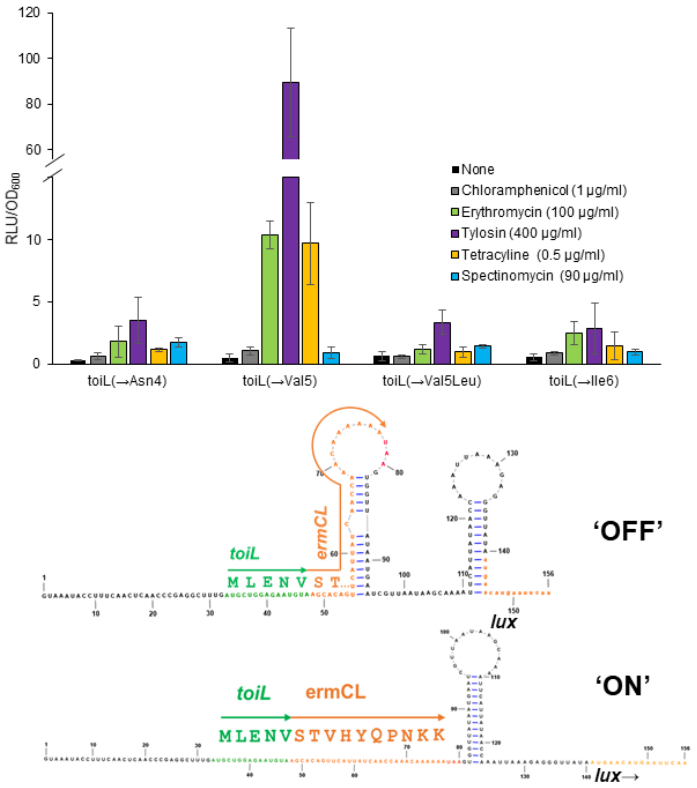

Figure 5. Ribosome stalling at the *topAI* leader. Luciferase activity of a hybrid *toiL-ermCL* stalling reporter (Bailey et al., 2008) fused to luciferase gene. Constructs included 261 nt *toiL* upstream sequence and up to the wild-type 4th, 5th or 6th codon or Val5Leu codon of *toiL* (as indicated on the *x*-axis). Truncated *toiL* was fused in frame to the 10th codon of *ermCL* and the remaining downstream sequence with alternating structural features. Schematic of the construct in an 'on' or 'off' state is depicted on the bottom. Bacterial cultures were grown in LB media until OD600~1.0 and the treated with indicated antibiotics. Luciferase activity was measured after 3h of treatment. Error bars represent ±1 standard deviation from the mean (n = 3).

strongly suggests that, in the presence of *topAI*-inducing drugs, the ribosome is arrested at a specific position – the 5th codon of *toiL* – and that the identity of the 5th codon contributes to stalling. Surprisingly, spectinomycin treatment did not cause an increase in expression of the stalling reporter; expression was similar to that of an untreated control or the non-inducing drug chloramphenicol (Fig. 5). As a control, we replaced *toiL* with the native *ermCL* sequence to show that this reporter is responsive to erythromycin treatment, but not other antibiotics (Fig. S3). Together, these data suggest that most of the *topAI* translation-upregulating drugs affect *topAI* expression by causing ribosome stalling at the 5th codon of *toiL*, whereas spectinomycin induces expression of *topAI* by a stalling-independent mechanism.

Discussion

toiL is a multipurpose sensory ORF

Our data indicate that *topAI* expression is regulated by translation of a uORF. Sensory uORFs are versatile tools that can be used to rapidly alter physiology in response to a wide variety of environmental stresses. Examples of genes regulated by uORFs include those involved in tryptophan biosynthesis (Yanofsky, 2007), Sigma factor regulation (Park et al., 2017), magnesium transport (Kriner and Groisman, 2015; Lee and Groisman, 2012; Park et al., 2010), putrescine production (Ben-Zvi et al., 2019), and antibiotic resistance (Lovett, 1996; Ramu et al., 2009). The common mechanism in these examples is always environmental signal-induced ribosome pausing at the uORF, which in turn leads to structural rearrangements in the downstream 5′ UTR. These structural rearrangements expose or mask an RBS (Ben-Zvi et al., 2019), intrinsic terminator (Oxender et al., 1979; Stauffer et al., 1978), or Rut (Figueroa-Bossi et al., 2014; Hollands et al., 2012; Kriner and Groisman, 2017), thereby regulating expression of the downstream gene. Thus, the general mode of *topAI* regulation resembles other examples of uORF-mediated translation and transcription attenuation. Given that uORF-mediated translational repression leads to premature Rho termination in *topAI*, it is intriguing to speculate that Rho prematurely terminates transcription of other uORF-regulated genes where the uORF modulates translation, such as *iraD* (Park et al., 2017), *erm* homologs (Ramu et al., 2009), *catA86* (Lovett, 1996) and *mgtCBR* (Choi et al., 2017).

We show that *toiL* senses ribosome inhibitors that exhibit very different modes of action (Fig. 2 and Fig. 5). Tylosin, erythromycin and tetracycline induce ribosome stalling at the 5th codon of *toiL*, and the codon identity (Val) is essential for the observed stalling effect (Fig. 5); by contrast, spectinomycin induces *topAI* translation that is dependent on *toiL* translation (Fig. 3B), but not ribosome stalling at *toiL* (Fig. 5). Molecules that occupy the ribosome exit tunnel have the potential to directly interact with amino acids in the nascent peptide, and thereby interfere with peptide elongation, leading to translation arrest. This has been shown for L-ornithine, L-tryptophan, and macrolide antibiotics; by binding in the ribosome exit tunnel, these molecules pause the ribosome in a nascent peptide sequence-dependent manner (Arenz et al., 2014b, 2014a; Bischoff et al., 2014; Valle et al., 2019). Macrolides such as erythromycin were suggested to restrict translation elongation of *ermBL/ermCL* uORFs, to prevent correct positioning of the next charged tRNA in the A-site and thus cause ribosome arrest (Arenz et al., 2014b, 2014a). The emerging ToiL nascent peptide (MLENV) could also be blocked by erythromycin and tylosin, as both have overlapping binding sites inside the exit tunnel of the ribosome (Hansen et al., 2002; Petropoulos et al., 2008; Poulsen et al., 2000). The induction of *ermB* or *ermC* genes does not always correlate with drug ability to cause ribosome arrest; these differences depend on the type of macrolide used and the specific codons of *ermBL* and *ermCL* ORFs (Dzyubak and Yap, 2016; Gupta et al., 2013a, 2016). It was surprising to see tylosin-induced stalling at *toiL*, since tylosin does not cause ribosome arrest at known erythromycin stalling sites (Bailey et al., 2008; Davis et al., 2014; Dzyubak and Yap, 2016). Perhaps the short length of the stalled *toiL* peptide (5 amino acids) allows for a better accommodation of the disaccharide branch of tylosin that extends towards the peptidyl transferase center (PTC) (Hansen et al., 2002), whereas that is unlikely with longer (9 or 10 amino acid) ErmCL/ErmBL nascent peptides (Arenz et al., 2014b, 2014a). The conformation of partial ToiL peptide in the exit tunnel is likely to make specific contacts with erythromycin and tylosin, leading to allosteric changes in the PTC, and subsequent ribosome arrest, as seen with *erm* genes. It would be interesting to see whether there are more *toiL*-like macrolide-inducible stalling motifs, and how they compare to those involved in regulation of *erm* genes (Ramu et al., 2009; Woolstenhulme et al., 2013).

Tetracycline and spectinomycin binding sites are in close proximity to each other on the 30S ribosome subunit, near the A-site (Borovinskaya et al., 2007; Brodersen et al., 2000). Both antibiotics mediated strong induction of *topAI*, but they appear to have a very different mechanism of action at *toiL* (Fig. 5). The fact that tetracycline does not make contacts with the exit tunnel of the ribosome and, presumably, the nascent peptide, but is dependent on the specific uORF codons for ribosome arrest, suggests that the mechanism of tetracycline-mediated translation inhibition might be more complex than previously thought. Chloramphenicol was shown to cause stalling at the leader ORF of chloramphenicol acetyltransferase gene *cat86A*. Chloramphenicol interacts with the ribosome on the 50S subunit near the A-site tRNA, thereby inhibiting the PTC (Wilson, 2014). The chloramphenicol-mediated ribosome stalling at the 5th codon of *cat86AL* was also dependent on one of the three amino acids in the penultimate position (Ala, Thr, Ser). The authors suggested that chloramphenicol might directly interact with the side chain of the specific amino acid in the A-site, but this needs further experimental

evidence (Lovett, 1996; Marks et al., 2016; Vázquez-Laslop and Mankin, 2018). We did not observe *topAI* induction by chloramphenicol (Fig. 5), consistent with *toiL* not encoding the preferred amino acids (Ala, Thr, Ser); however, similar to regulation of *cat86AL* by chloramphenicol, tetracycline could interact directly or indirectly with Val5 of ToiL in the P-site. How the spectinomycin-modified ribosome works at *toiL* without an apparent stalling mechanism to upregulate *topAI* remains an open question.

It is likely that the *toiL-topAI-yjhQ* system has evolved to respond to low levels of antibiotics to quickly alter the metabolic state of the cell and prevent excessive damage by high concentrations of drugs that would inhibit all protein synthesis (Gupta et al., 2013b). The example of ToiL and others shows how uORFs can be used to sense a wide range of translational stresses in a manner dependent on the sequence of the uORF nascent peptide. The detection specificity of the nascent peptide can be modified by the identity of the codons, and the number of codons used; thus, it is likely that many combinations of drugs and uORF sequences could lead to translational pausing. The post-translational regulatory nature of these ORFs ensures a rapid response to changing environmental conditions, and the small size of the uORF preserves energy expenditure. With the recent identification of large numbers of uORFs in diverse bacterial species (Shell et al., 2015; Weaver et al., 2019), it will be exciting to see what other types of sensory capabilities they encode.

Translation attenuation and premature Rho-dependent termination

Our data suggest that Rho-dependent termination at *topAI* is a consequence of *topAI* translational repression (Fig. 2). Other studies of premature termination events within coding regions suggested that termination occurs due to the unmasking of Ruts within the ORF that are usually occluded by translating ribosomes (Bastet et al., 2017; Ben-Zvi et al., 2019; Bossi et al., 2012). By contrast, we showed that the Rut for *topAI* is located within the 5′ UTR. This suggests that the mechanism by which translation of *topAI* prevents Rho termination is distinct to that at other characterized examples of prematurely Rho-terminated genes. Specifically, ribosomes translating *topAI* likely prevent Rho from catching the elongating RNAP, rather than preventing Rho loading onto the nascent RNA. If there are indeed two distinct mechanisms by which ribosomes can prevent Rho termination, it suggests that the level of translation required for each mechanism may be different. An alternative possibility is that the *topAI* Rut is very long and extends into the *topAI* ORF, in which case ribosomes would prevent Rho termination by preventing Rho loading.

We identified elements of the *topAI* Rut that are located a short distance upstream of *toiL*. Given the length of RNA required to constitute a Rut, the *topAI* Rut must overlap *toiL*. Thus, the Rut is functional despite the presence of an actively translated overlapping ORF (Fig. 1, S2B). We propose that (i) Rho can only load onto the *topAI* 5′ UTR after translation of *toiL* is terminated, or (ii) Rho can loop the RNA around the *toiL* region to access upstream and downstream elements of the Rut. It has previously been proposed that Rho can step over an RNA roadblock to access available Ruts (Kriner and Groisman, 2017; Schwartz et al., 2007), thereby helping Rho to overcome roadblocks at the 5′ UTR, such as the *toiL* ORF.

Complex regulation of *topAI-yjhQ* toxin-antitoxin operon

To the best of our knowledge, *topAI-yjhQ* is the first toxin-antitoxin system shown to be regulated by a uORF and premature Rho termination. The arrangement of the *topAI-yjhQ* operon is unusual because antitoxin genes are typically located upstream of toxin genes, such that the antitoxin is expressed early enough to counteract toxin activity (Page and Peti, 2016). Uncontrolled overexpression of TopAI toxin would inhibit Topoisomerase A activity and cause excessive negative supercoiling (Rovinskiy et al., 2012; Yamaguchi and Inouye, 2015). uORF-mediated regulation may have evolved to ensure that the toxin is repressed under normal growth conditions, with subsequent Rho-termination preventing unproductive transcription. At the same time, post-transcriptional regulation and the sensitivity of the uORF to sub-inhibitory drug concentrations would allows for rapid induction of the toxin-antitoxin system, and physiological adaptation to evade inhibitory drug effects. Antibiotics target active cellular processes, and toxin-antitoxin systems can protect the cell from antibiotic-induced damage (Harms et al., 2016). Ours and other published transcriptomic data suggest that *toiL-topAI-yjhQ* and the downstream *yjhP* gene are in an operon, and are all upregulated upon Rho inhibition or exposure to inducing antibiotics (Dzyubak and Yap, 2016; Peters et al., 2012). If this is a true toxin-antitoxin system, then there must be an additional post-translational regulation for the antitoxin product YjhQ. The role of YjhP, a predicted methyltransferase, is also unclear. Overexpression of TopAI in the absence of YjhQ caused cell death (Yamaguchi and Inouye, 2015). Physiological levels of TopAI are likely to be much lower even upon induction of the system, as we

have never observed TopAI-related growth inhibition in our study; however, the cellular function of TopAI is beyond the scope of this work.

Materials and Methods

Strains and plasmids.

All strains, plasmids and oligonucleotides used in this study are listed in Supplementary Tables 4 and 5, respectively. *E. coli* MG1655 Δ*lacZ* Δ*topAI/Q*::*thyA* (GB001) strain was constructed using the 'Flexible Recombineering Using Integration of *thyA*' (FRUIT) method (Stringer et al., 2012). Briefly, *thyA* gene was amplified with JW7676 + JW7677 primers and electroporated into AMD189 to replace *topAI* gene from 400 nt upstream to 90 nt of the *yjhQ* coding region (Stringer et al., 2012).

All *topAI* region-containing plasmids (pJTW100, pGB164, pGB182, pGB196, pGB197, pGB200, pGB201, pGB202, pGB215, pGB217, pGB297, pGB305, pGB306, pGB313) were made to include sequence starting at -400 nt upstream of *topAI* and were driven by a native *topAI* promoter. For gene-*lacZ* fusions, the pAMD-BA-*lacZ* (Stringer et al., 2014) backbone was used. Plasmids for luciferase assays were constructed by cloning the region of interest into a pGB135 plasmid. pGB135 was made by cloning JW8044 + JW8522 and JW8523 + JW8047 primer products into the XhoI and XbaI sites of pCS-PesaRlux (Shong and Collins, 2013). pGB135 has the P*esaR* fragment replaced with an excisable *E. coli* high expression promoter and convenient restriction sites for transcriptional or translation fusions to the *luxC* gene. The entire *luxCDABE* operon is encoded in pGB135. 'Transcriptional' reporter fusions included an RBS of the reporter, whereas 'translational' fusions used the RBS up to the initiation codon of the gene of interest followed by the first codon of the reporter gene.

Plasmid pJTW100 included a full-length *topAI* gene and *yjhQ* region up to 90 nt (primers JW5638 + JW5639) into the coding sequence that is translationally fused to *lacZ*. Plasmids pGB215, pGB217 were made by cloning a truncated *topAI* gene up to 10 or 42 nt (primers JW5638 + JW9453 or JW9154) of the coding sequence with an in-frame stop codon 'TAA' as a transcriptional fusion to *lacZ*. Plasmids pGB305 and pGB306 additionally had a mutated *rut* in the 5′ UTR (4C → 4A) that were amplified with primers JW5638 + JW9453/JW9154 from the pGB299 template. Construct pGB299 with a full-length *topAI-lacZ* fusion and *rut** was made with JW5638, JW8023 and mutagenic JW9803/JW9804 primers. Construct pGB214 was equivalent to pJTW100 and carried a mutation in the 5′ UTR (*toiL* ATG→gTa) that was introduced with mutagenic primers JW9106/JW9107. pGB182 (wild-type) and pGB297 (*toiL* ATG→gTa) included the *topAI* 5′ UTR that was transcriptionally fused to *lacZ* using primer products JW5638 + JW8809 and wild-type MG1655 or pGB214 as templates for amplification. Plasmid pGB164 was made by cloning the entire *toiL* sequence as a translational fusion to *lacZ* with primers JW5638 + JW8741. Plasmids pGB196, pGB197, pGB200, pGB201 additionally carried *toiL* codon mutations as indicated in Fig. 3A that were introduced by mutagenic PCR primers JW8999, JW8998, JW9013, JW9014. Plasmids pGB202 and pGB313 were made by cloning a wild-type version of *topAI* 5′ UTR (pGB202) or *toiL* (ATG→gTa) mutated version into a pGB135 plasmid as a translational fusion to *luxC* gene using primer products JW9288 + JW9289 and wild-type MG1655 or pGB214 as templates for amplification. Plasmids pGB324, pGB326, pGB327, pGB328 included the same *topAI* upstream region as the aforementioned plasmids up to the indicated *toiL* codon in Fig. 5; these plasmids were made with primer products JW9288 + JW10122/10145/10146/10147 and JW10123 + JW9965. These regions were fused in-frame with the *ermCL* gene from the 10th codon that was followed by a regulatory *ermC* region (Bailey et al., 2008) and translationally fused to *luxC*. The sequence of *toiL* upstream region and *ermC* regulatory region is provided in Supplementary Table 5 as the geneBlock GB007. pGB308 was constructed the same way but *toiL* coding sequenced was replaced with the beginning of the *ermCL* sequence (1-9th codon) as a control (Fig. S3). Plasmids pGB322 and pGB318 were constructed cloning a complete rRNA operon from TSS (JW10036) to the last tRNA (JW10037) into a propionate inducible vector pPro24 (Lee and Keasling, 2005). Plasmid pGB318 contained a ΔT1917 mutation in the 23S rRNA gene that was introduced with mutagenic primers JW9737/JW9740. Plasmid pGB322 was created by using pGB318 as a template and restoring ΔT1917 mutation into a wt 23S rRNA with mutagenic primers JW10104/JW10105. Both wt (pGB322) and mutant (pGB318) operons were a hybrid of rRNA 'B' (upstream of the 23S gene position +1917) and 'C' (downstream of the 23S gene position +1917) operons, but the wild-type version had no effect on *topAI* expression (Fig. 2). Rho-dependent transcription termination reporter plasmid pGB72 was constructed by cloning a high expression promoter (Burr et al., 2000) followed by a known Rho terminator (568 nt of a reverse-complemented *Hin*dIII fragment from the *rrsB* gene (Li et al., 1984)), into the *Xho*I and *Bam*HI restriction sites of the pET-P*esaR-lux* plasmid (Shong and Collins, 2013) using primer pairs JW7977b + JW7979b and JW7994 + JW7995.

Isolation and identification of trans-acting mutants

The trans-acting mutant genetic selection was performed as described in Baniulyte et al, 2017. Briefly, a MG1655 Δ*lacZ* strain with pJTW100 was used. Bacterial cultures were grown at 37 °C in LB medium. 100 µl of an overnight culture was washed and plated on M9+0.2% lactose agar. Spontaneous survivors were tested for increased plasmid copy number and *topAI cis*-mutations and eliminated if positive. Chromosomal mutations were identified either by PCR amplification and sequencing of *rho* or by whole genome sequencing. Rho mutants were also detected by transducing a wild-type *rho* locus and looking for phenotype reversion, or by introducing and assaying a Rho-dependent termination reporter plasmid (pGB72).

SHAPE-seq

A total of three biological replicates of the strain GB001 + pJTW100 were grown to an OD_{600} of ~1.2 in LB medium at 37 °C.

Cultures were split, and one set of two replicates were treated with 0.2 μg/ml tetracycline (T3383, Sigma) for 90 min. Cultures were subjected to the in-cell SHAPE-seq procedure previously described for poorly expressed mRNAs (Watters et al., 2016a). The SHAPE reagent 1M7 was purchased from MedChem Express (HY-D0913). SHAPE-seq libraries was sequenced using an Illumina MiSeq instrument (251 bp, pair-end reads). Sequencing data were analyzed using the spats pipeline (Watters et al., 2016b, 2016a). Raw reactivities are listed in Supplementary Table 3. Significant changes in reactivity and corresponding adjusted *p*-values upon tetracycline treatment were determined using the DESeq2 R package (Love et al., 2014), comparing untreated and tetracycline treated sample reactivities at each position using 3 ('Untreated') and 2 ('Treated') biological replicates from each sample. Structures in Fig. 5 were drawn using StructureEditor (DH Mathews Lab).

Reporter assays

Cultures for luciferase or β-galactosidase assays were grown at 37 °C in LB medium to an OD_{600} of 0.5–0.6 or OD_{600} of 1.0-1.2, as indicated in the figure legends. Tetracycline (Sigma #T3383), spectinomycin (Sigma #S4014), erythromycin (Sigma #E5389) or tylosin (Sigma #T6134) antibiotics were added at indicated concentrations and timepoints. β-galactosidase assays were performed as previously described (Baniulyte et al., 2017). For luciferase assays, each cell culture (200 μl) was aliquoted into a 96-well plate with four technical replicates each. Luminescence readings were taken using a Biotek Synergy 2 instrument. Luminescence counts (RLU) were adjusted for OD_{600} and reported as RLU/OD_{600}. Antibiotic concentrations and length of treatments are indicated in the figure legends.

References:

Adhya, S., and Gottesman, M. (1978). Control of Transcription Termination. Annu. Rev. Biochem. *47*, 967–996.

Agrawal, R.K., Sharma, M.R., Kiel, M.C., Hirokawa, G., Booth, T.M., Spahn, C.M.T., Grassucci, R. a, Kaji, A., and Frank, J. (2004). Visualization of ribosome-recycling factor on the Escherichia coli 70S ribosome: functional implications. Proc. Natl. Acad. Sci. U. S. A. *101*, 8900–8905.

Alifano, P., Rivellini, F., Limauro, D., Bruni, C.B., and Carlomagno, M.S. (1991). A consensus motif common to all rho-dependent prokaryotic transcription terminators. Cell *64*, 553–563.

Arenz, S., Ramu, H., Gupta, P., Berninghausen, O., Beckmann, R., Vázquez-Laslop, N., Mankin, A.S., and Wilson, D.N. (2014a). Molecular basis for erythromycin-dependent ribosome stalling during translation of the ErmBL leader peptide. Nat. Commun. *5*.

Arenz, S., Meydan, S., Starosta, A.L., Berninghausen, O., Beckmann, R., Vázquez-Laslop, N., and Wilson, D.N. (2014b). Drug sensing by the ribosome induces translational arrest via active site perturbation. Mol. Cell *56*, 446–452.

Baek, J., Lee, J., Yoon, K., and Lee, H. (2017). Identification of Unannotated Small Genes in Salmonella. G3 Genes, Genomes, Genet. *7*, 983–989.

Bailey, M., Chettiath, T., and Mankin, A.S. (2008). Induction of erm(C) expression by noninducing antibiotics. Antimicrob. Agents Chemother. *52*, 866–874.

Baniulyte, G., Singh, N., Benoit, C., Johnson, R., Ferguson, R., Paramo, M., Stringer, A.M., Scott, A., Lapierre, P., and Wade, J.T. (2017). Identification of regulatory targets for the bacterial Nus factor complex. Nat. Commun. *8*, 2027.

Barat, C., Datta, P.P., Raj, V.S., Sharma, M.R., Kaji, H., Kaji, A., and Agrawal, R.K. (2007). Progression of the Ribosome Recycling Factor through the Ribosome Dissociates the Two Ribosomal Subunits. Mol. Cell *27*, 250–261.

Bastet, L., Chauvier, A., Singh, N., Lussier, A., Lamontagne, A.-M., Prévost, K., Massé, E., Wade, J.T., and Lafontaine, D.A. (2017). Translational control and Rho-dependent transcription termination are intimately linked in riboswitch regulation. Nucleic Acids Res. *45*, 7474–7486.

Ben-Zvi, T., Pushkarev, A., Seri, H., Elgrably-Weiss, M., Papenfort, K., and Altuvia, S. (2019). mRNA dynamics and alternative conformations adopted under low and high arginine concentrations control polyamine biosynthesis in Salmonella. PLoS Genet. *15*, e1007646.

Bischoff, L., Berninghausen, O., and Beckmann, R. (2014). Molecular Basis for the Ribosome Functioning as an L-Tryptophan Sensor. Cell Rep. *9*, 469–475.

Borovinskaya, M.A., Shoji, S., Holton, J.M., Fredrick, K., and Cate, J.H.D. (2007). A steric block in translation caused by the antibiotic spectinomycin. ACS Chem. Biol. *2*, 545–552.

Bossi, L., Schwartz, A., Guillemardet, B., Boudvillain, M., and Figueroa-Bossi, N. (2012). A role for Rho-dependent polarity in gene regulation by a noncoding small RNA. Genes Dev. *26*, 1864–1873.

Breaker, R.R. (2018). Riboswitches and Translation Control. Cold Spring Harb. Perspect. Biol. *10*, a032797.

Brodersen, D.E., Clemons, W.M., Carter, A.P., Morgan-Warren, R.J., Wimberly, B.T., and Ramakrishnan, V. (2000). The structural basis for the action of the antibiotics tetracycline, pactamycin, and hygromycin B on the 30S ribosomal subunit. Cell *103*, 1143–1154.

Burmann, B.M., Schweimer, K., Luo, X., Wahl, M.C., Stitt, B.L., Gottesman, M.E., and Rosch, P. (2010). A NusE:NusG Complex Links Transcription and Translation. Science (80-.). *328*, 501–504.

Burns, C.M., and Richardson, J.P. (1995). NusG is required to overcome a kinetic limitation to Rho function at an intragenic terminator. Proc. Natl. Acad. Sci. U. S. A. *92*, 4738–4742.

Burr, T., Mitchell, J., Kolb, A., Minchin, S., and Busby, S. (2000). DNA sequence elements located immediately upstream of the -10 hexamer in Escherichia coli promoters: a systematic study. Nucleic Acids Res. *28*, 1864–1870.

Cardinale, C.J., Washburn, R.S., Tadigotla, V.R., Brown, L.M., Gottesman, M.E., and Nudler, E. (2008). Termination factor Rho and its cofactors NusA and NusG silence foreign DNA in E. coli. Science *320*, 935–938.

Caron, M.-P., Bastet, L., Lussier, A., Simoneau-Roy, M., Massé, E., and Lafontaine, D.A. (2012). Dual-acting riboswitch control of translation initiation and mRNA decay. Proc. Natl. Acad. Sci. U. S. A. *109*, E3444-53.

Chalissery, J., Muteeb, G., Kalarickal, N.C., Mohan, S., Jisha, V., and Sen, R. (2011). Interaction surface of the transcription terminator rho required to form a complex with the C-terminal domain of the antiterminator NusG. J. Mol. Biol.

Chhakchhuak, P.I.R., Khatri, A., and Sen, R. (2018). Mechanism of Action of Bacterial Transcription Terminator Rho. Proc. Indian Natl. Sci. Acad.

Choi, E., Choi, S., Nam, D., Park, S., Han, Y., Lee, J.-S., and Lee, E.-J. (2017). Elongation factor P restricts Salmonella's growth by controlling translation of a Mg2+ transporter gene during infection. Sci. Rep. *7*, 42098.

Dar, D., and Sorek, R. (2018). High-resolution RNA 3-ends mapping of bacterial Rho-dependent transcripts. Nucleic Acids Res.

Davis, A.R., Gohara, D.W., and Yap, M.-N.F. (2014). Sequence selectivity of macrolide-induced translational attenuation. Proc. Natl. Acad. Sci. *111*, 15379–15384.

Dzyubak, E., and Yap, M.-N.F. (2016). The expression of antibiotic resistance methyltransferase correlates with mRNA stability independently of ribosome stalling. Antimicrob. Agents Chemother. *60*, AAC.01806-16.

Fan, H., Conn, A.B., Williams, P.B., Diggs, S., Hahm, J., Gamper, H.B., Hou, Y.M., O'Leary, S.E., Wang, Y., and Blaha, G.M. (2017). Transcription-Translation coupling: Direct interactions of RNA polymerase with ribosomes and ribosomal subunits. Nucleic Acids Res. *45*, 11043–11055.

Figueroa-Bossi, N., Schwartz, A., Guillemardet, B., D'Heygère,

F., Bossi, L., and Boudvillain, M. (2014). RNA remodeling by bacterial global regulator CsrA promotes Rho-dependent transcription termination. Genes Dev. *28*, 1239–1251.

Gupta, P., Kannan, K., Mankin, A., and Vázquez-Laslop, N. (2013a). Regulation of gene expression by macrolide-induced ribosomal frameshifting. Mol. Cell *52*, 629–642.

Gupta, P., Sothiselvam, S., Vázquez-Laslop, N., and Mankin, A.S. (2013b). Deregulation of translation due to post-transcriptional modification of rRNA explains why erm genes are inducible. Nat. Commun. *4*, 1984.

Gupta, P., Liu, B., Klepacki, D., Gupta, V., Schulten, K., Mankin, A.S., and Vázquez-Laslop, N. (2016). Nascent peptide assists the ribosome in recognizing chemically distinct small molecules. Nat. Chem. Biol. *12*, 153–158.

Hansen, J.L., Ippolito, J.A., Ban, N., Nissen, P., Moore, P.B., and Steitz, T.A. (2002). The structures of four macrolide antibiotics bound to the large ribosomal subunit. Mol. Cell *10*, 117–128.

Harms, A., Maisonneuve, E., and Gerdes, K. (2016). Mechanisms of bacterial persistence during stress and antibiotic exposure. Science (80-.).

Hart, C.M., and Roberts, J.W. (1991). Rho-dependent transcription termination. Characterization of the requirement for cytidine in the nascent transcript. J. Biol. Chem. *266*, 24140–24148.

Hollands, K., Proshkin, S., Sklyarova, S., Epshtein, V., Mironov, A., Nudler, E., and Groisman, E. a. (2012). Riboswitch control of Rho-dependent transcription termination. Proc. Natl. Acad. Sci. U. S. A. *109*, 5376–5381.

Kohler, R., Mooney, R.A., Mills, D.J., Landick, R., and Cramer, P. (2017). Architecture of a transcribing-translating expressome. Science (80-.). *356*, 194–197.

Koslover, D.J., Fazal, F.M., Mooney, R.A., Landick, R., and Block, S.M. (2012). Binding and translocation of termination factor rho studied at the single-molecule level. J. Mol. Biol. *423*, 664–676.

Kriner, M.A., and Groisman, E.A. (2015). The Bacterial Transcription Termination Factor Rho Coordinates Mg(2+) Homeostasis with Translational Signals. J. Mol. Biol. *427*, 3834–3849.

Kriner, M.A., and Groisman, E.A. (2017). RNA secondary structures regulate three steps of Rho-dependent transcription termination within a bacterial mRNA leader. Nucleic Acids Res. *45*, 631–642.

Kriner, M.A., Sevostyanova, A., and Groisman, E.A. (2016). Learning from the Leaders: Gene Regulation by the Transcription Termination Factor Rho. Trends Biochem. Sci. *41*, 690–699.

Lawson, M.R., Dyer, K., and Berger, J.M. (2016). Ligand-induced and small-molecule control of substrate loading in a hexameric helicase. Proc. Natl. Acad. Sci. *113*, 13714–13719.

Lee, E.-J.J., and Groisman, E.A. (2012). Tandem attenuators control expression of the Salmonella mgtCBR virulence operon. Mol. Microbiol. *86*, 212–224.

Lee, S.K., and Keasling, J.D. (2005). A propionate-inducible expression system for enteric bacteria. Appl. Environ. Microbiol.

Li, S.C., Squires, C.L., and Squires, C. (1984). Antitermination of E. coli rRNA transcription is caused by a control region segment containing lambda nut-like sequences. Cell *38*, 851–860.

Love, M.I., Huber, W., and Anders, S. (2014). Moderated estimation of fold change and dispersion for RNA-seq data with DESeq2. Genome Biol. *15*, 550.

Lovett, P.S. (1996). Translation attenuation regulation of chloramphenicol resistance in bacteria--a review. Gene *179*, 157–162.

Marks, J., Kannan, K., Roncase, E.J., Klepacki, D., Kefi, A., Orelle, C., Vázquez-Laslop, N., and Mankin, A.S. (2016). Context-specific inhibition of translation by ribosomal antibiotics targeting the peptidyl transferase center. Proc. Natl. Acad. Sci. *113*, 12150–12155.

Martinez, A., Opperman, T., and Richardson, J.P. (1996). Mutational analysis and secondary structure model of the RNP1-like sequence motif of transcription termination factor Rho. J. Mol. Biol. *257*, 895–908.

McGary, K., and Nudler, E. (2013). RNA polymerase and the ribosome: the close relationship. Curr. Opin. Microbiol. *16*, 112–117.

Nadiras, C., Eveno, E., Schwartz, A., Figueroa-Bossi, N., and Boudvillain, M. (2018). A multivariate prediction model for Rho-dependent termination of transcription. Nucleic Acids Res. *46*, 8245–8260.

Oxender, D.L., Zurawski, G., and Yanofsky, C. (1979). Attenuation in the Escherichia coli tryptophan operon: role of RNA secondary structure involving the tryptophan codon region. Proc. Natl. Acad. Sci. U. S. A. *76*, 5524–5528.

Page, R., and Peti, W. (2016). Toxin-antitoxin systems in bacterial growth arrest and persistence. Nat. Chem. Biol. *12*, 208–214.

Park, H., McGibbon, L.C., Potts, A.H., Yakhnin, H., Romeo, T., and Babitzke, P. (2017). Translational Repression of the RpoS Antiadapter IraD by CsrA Is Mediated via Translational Coupling to a Short Upstream Open Reading Frame. MBio *8*.

Park, S.-Y., Cromie, M.J., Lee, E.-J., and Groisman, E.A. (2010). A bacterial mRNA leader that employs different mechanisms to sense disparate intracellular signals. Cell *142*, 737–748.

Peters, J.M., Mooney, R.A., Kuan, P.F., Rowland, J.L., Keles, S., and Landick, R. (2009). Rho directs widespread termination of intragenic and stable RNA transcription. Proc. Natl. Acad. Sci. U. S. A. *106*, 15406–15411.

Peters, J.M., Mooney, R.A., Grass, J.A., Jessen, E.D., Tran, F., and Landick, R. (2012). Rho and NusG suppress pervasive antisense transcription in Escherichia coli. Genes Dev. *26*, 2621–2633.

Petropoulos, A.D., Kouvela, E.C., Dinos, G.P., and Kalpaxis, D.L. (2008). Stepwise binding of tylosin and erythromycin to Escherichia coli ribosomes, characterized by kinetic and footprinting analysis. J. Biol. Chem. *283*, 4756–4765.

Poulsen, S.M., Kofoed, C., and Vester, B. (2000). Inhibition of

the ribosomal peptidyl transferase reaction by the mycarose moiety of the antibiotics carbomycin, spiramycin and tylosin. J. Mol. Biol. *304*, 471–481.

Proshkin, S., Rahmouni, A.R., Mironov, A., and Nudler, E. (2010). Cooperation between translating ribosomes and RNA polymerase in transcription elongation. Science *328*, 504–508.

Ramu, H., Mankin, A., and Vazquez-Laslop, N. (2009). Programmed drug-dependent ribosome stalling: MicroReview. Mol. Microbiol. *71*, 811–824.

Ray-Soni, A., Bellecourt, M.J., and Landick, R. (2016). Mechanisms of Bacterial Transcription Termination: All Good Things Must End. Annu. Rev. Biochem. *85*, 319–347.

Richardson, J.P. (2002). Rho-dependent termination and ATPases in transcript termination. Biochim. Biophys. Acta *1577*, 251–260.

Rivellini, F., Alifano, P., Piscitelli, C., Blasi, V., Bruni, C.B., Carlomagno, M.S., Brunt, C.B., and Carlomagno, M.S. (1991). A cytosine- over guanosine-rich sequence in RNA activates rho-dependent transcription termination. Mol. Microbiol. *5*, 3049–3054.

Roberts, J.W. (2019). Mechanisms of Bacterial Transcription Termination. J. Mol. Biol.

Rovinskiy, N., Agbleke, A.A., Chesnokova, O., Pang, Z., and Higgins, N.P. (2012). Rates of gyrase supercoiling and transcription elongation control supercoil density in a bacterial chromosome. PLoS Genet. *8*, e1002845.

Saxena, S., Myka, K.K., Washburn, R., Costantino, N., Court, D.L., and Gottesman, M.E. (2018). Escherichia coli transcription factor NusG binds to 70S ribosomes. Mol. Microbiol. *108*, 495–504.

Schneider, D., Gold, L., and Platt, T. (1993). Selective Enrichment of Rna Species for Tight-Binding to Escherichia-Coli Rho-Factor. Faseb J. *7*, 201–207.

Schwartz, A., Walmacq, C., Rahmouni, A.R., and Boudvillain, M. (2007). Noncanonical interactions in the management of RNA structural blocks by the transcription termination rho helicase. Biochemistry *46*, 9366–9379.

Sedlyarova, N., Shamovsky, I., Bharati, B.K., Epshtein, V., Chen, J., Gottesman, S., Schroeder, R., and Nudler, E. (2016). sRNA-Mediated Control of Transcription Termination in E. coli. Cell *167*, 111-121.e13.

Shashni, R., Qayyum, M.Z., Vishalini, V., Dey, D., and Sen, R. (2014). Redundancy of primary RNA-binding functions of the bacterial transcription terminator Rho. Nucleic Acids Res. *42*, 9677–9690.

Shell, S.S., Wang, J., Lapierre, P., Mir, M., Chase, M.R., Pyle, M.M., Gawande, R., Ahmad, R., Sarracino, D.A., Ioerger, T.R., et al. (2015). Leaderless Transcripts and Small Proteins Are Common Features of the Mycobacterial Translational Landscape. PLoS Genet. *11*, e1005641.

Shong, J., and Collins, C.H. (2013). Engineering the esaR promoter for tunable quorum sensing- dependent gene expression. ACS Synth. Biol. *2*, 568–575.

Silva, I.J., Barahona, S., Eyraud, A., Lalaouna, D., Figueroa-Bossi, N., Massé, E., and Arraiano, C.M. (2019). SraL sRNA interaction regulates the terminator by preventing premature transcription termination of rho mRNA. Proc. Natl. Acad. Sci. *116*, 3042–3051.

Skordalakes, E., and Berger, J.M. (2006). Structural insights into RNA-dependent ring closure and ATPase activation by the Rho termination factor. Cell *127*, 553–564.

de Smit, M.H., Verlaan, P.W.G., van Duin, J., and Pleij, C.W.A. (2009). In Vivo Dynamics of Intracistronic Transcriptional Polarity. J. Mol. Biol. *385*, 733–747.

Stauffer, G. V, Zurawski, G., and Yanofsky, C. (1978). Single base-pair alterations in the Escherichia coli trp operon leader region that relieve transcription termination at the trp attenuator. Proc. Natl. Acad. Sci. *75*, 4833–4837.

Stringer, A.M., Singh, N., Yermakova, A., Petrone, B.L., Amarasinghe, J.J., Reyes-Diaz, L., Mantis, N.J., and Wade, J.T. (2012). FRUIT, a scar-free system for targeted chromosomal mutagenesis, epitope tagging, and promoter replacement in Escherichia coli and Salmonella enterica. PLoS One *7*, e44841.

Stringer, A.M., Currenti, S., Bonocora, R.P., Baranowski, C., Petrone, B.L., Palumbo, M.J., Reilly, A.A., Zhang, Z., Erill, I., and Wade, J.T. (2014). Genome-scale analyses of Escherichia coli and Salmonella enterica AraC reveal noncanonical targets and an expanded core regulon. J. Bacteriol. *196*, 660–671.

Subramanian, S.L., Ramu, H., and Mankin, A.S. (2012). Inducible resistance to macrolide antibiotics. In Antibiotic Discovery and Development, (Boston, MA: Springer US), pp. 455–484.

Thomason, M.K., Bischler, T., Eisenbart, S.K., F??rstner, K.U., Zhang, A., Herbig, A., Nieselt, K., Sharma, C.M., and Storza, G. (2015). Global transcriptional start site mapping using differential RNA sequencing reveals novel antisense RNAs in Escherichia coli. J. Bacteriol. *197*, 18–28.

Thomsen, N.D., Lawson, M.R., Witkowsky, L.B., Qu, S., and Berger, J.M. (2016). Molecular mechanisms of substrate-controlled ring dynamics and substepping in a nucleic acid-dependent hexameric motor. Proc. Natl. Acad. Sci. *113*, E7691–E7700.

Valle, A.H. del, Seip, B., Cervera-Marzal, I., Sacheau, G., Seefeldt, A.C., and Innis, C.A. (2019). Ornithine capture by a translating ribosome controls bacterial polyamine synthesis. BioRxiv 604074.

Vázquez-Laslop, N., and Mankin, A.S. (2018). Context-Specific Action of Ribosomal Antibiotics. Annu. Rev. Microbiol. *72*, 185–207.

Wang, J., Rennie, W., Liu, C., Carmack, C.S., Prévost, K., Caron, M.-P., Massé, E., Ding, Y., and Wade, J.T. (2015a). Identification of bacterial sRNA regulatory targets using ribosome profiling. Nucleic Acids Res. *43*, 10308–10320.

Wang, X., Ji, S.C., Jeon, H.J., Lee, Y., and Lim, H.M. (2015b). Two-level inhibition of galK expression by Spot 42: Degradation of mRNA mK2 and enhanced transcription termination before the galK gene. Proc. Natl. Acad. Sci. U. S. A. *112*, 7581–7586.

Watters, K.E., Abbott, T.R., and Lucks, J.B. (2016a). Simultaneous characterization of cellular RNA structure and

function with in-cell SHAPE-Seq. Nucleic Acids Res. *44*, e12.

Watters, K.E., Yu, A.M., Strobel, E.J., Settle, A.H., and Lucks, J.B. (2016b). Characterizing RNA structures in vitro and in vivo with selective 2'-hydroxyl acylation analyzed by primer extension sequencing (SHAPE-Seq). Methods *103*, 34–48.

Weaver, J., Mohammad, F., Buskirk, A.R., and Storz, G. (2019). Identifying Small Proteins by Ribosome Profiling with Stalled Initiation Complexes. MBio *10*.

Wilson, D.N. (2014). Ribosome-targeting antibiotics and mechanisms of bacterial resistance. Nat. Rev. Microbiol. *12*, 35–48.

Woolstenhulme, C.J., Parajuli, S., Healey, D.W., Valverde, D.P., Petersen, E.N., Starosta, A.L., Guydosh, N.R., Johnson, W.E., Wilson, D.N., and Buskirk, A.R. (2013). Nascent peptides that block protein synthesis in bacteria. Proc. Natl. Acad. Sci. *110*, E878–E887.

Yamaguchi, Y., and Inouye, M. (2015). An endogenous protein inhibitor, YjhX (TopAI), for topoisomerase i from Escherichia coli. Nucleic Acids Res. *43*, 10387–10396.

Yanofsky, C. (2007). RNA-based regulation of genes of tryptophan synthesis and degradation, in bacteria. RNA *13*, 1141–1154.

Zhu, A.Q., and von Hippel, P.H. (1998a). Rho-dependent termination within the trp t' terminator. I. Effects of rho loading and template sequence. Biochemistry *37*, 11202–11214.

Zhu, A.Q., and von Hippel, P.H. (1998b). Rho-dependent termination within the trp t' terminator. II. Effects of kinetic competition and rho processivity. Biochemistry *37*, 11215–11222.

Zuker, M. (2003). Mfold web server for nucleic acid folding and hybridization prediction. Nucleic Acids Res. *31*, 3406–3415.